Renewable Energy 114 (2017) 1005–1012

Contents lists available at ScienceDirect

Renewable Energy

journal homepage: www.elsevier.com/locate/renene

Thermodynamic analysis of the drying process of bananas in a small-scale solar updraft tower in Brazil

Cristiana Brasil Maia [a, *], André Guimarães Ferreira [b], Luben Cabezas-Gómez [c], Janaína de Oliveira Castro Silva [a], Sérgio de Morais Hanriot [a]

[a] Department of Mechanical Engineering, Pontifícia Universidade Católica de Minas Gerais, Belo Horizonte, Brazil
[b] Graduate Program of Energy Engineering, Centro Federal de Educação Tecnológica de Minas Gerais, Belo Horizonte, Brazil
[c] Department of Mechanical Engineering, São Carlos School of Engineering, University of São Paulo, São Carlos, Brazil

A R T I C L E I N F O

Article history:
Received 5 December 2016
Received in revised form
12 April 2017
Accepted 25 July 2017
Available online 26 July 2017

Keywords:
Solar updraft tower
Exergetic analysis
Drying

A B S T R A C T

This paper presents a thermodynamic analysis of the drying of bananas inside a small-scale prototype solar updraft tower in Belo Horizonte, Brazil. A model based on the first and second laws of thermodynamics was developed, using the ambient conditions and airflow parameters data obtained in the experimental prototype. The exergy rates were determined, and it was concluded that the incident solar radiation plays an important role on the drying process of bananas, the higher the solar radiation, the higher the exergy rates. The exergetic efficiency was compared to that obtained without products inside the solar updraft tower, and it was found that the exergetic efficiency increased from about 20% to 27% with load.

1. Introduction

With the rapid consumption of fossil energy and changes to the global climate, renewable energy technologies have become important. Solar updraft towers represent a possible use of solar energy to generate a solar induced convective airflow. The basic idea of the device is to combine the greenhouse and the chimney effects. It consists of three main components: a solar collector, a tower, and wind turbines. The incident solar radiation heats the soil under the collector, which heats the air. Through buoyancy forces, the hot air rises and flows into the chimney. The air updraft can be used to drive wind turbines connected to an electrical generator.

The first prototype was built in Manzanares in 1981/1982 and proved to be reliable and technically viable [1]. Since Manzanares project, several studies have been conducted, both experimentally and theoretically. Several experimental prototypes were built in Iran. Najmi et al. [2] evaluated the use of different materials at the collector bottom in order to produce more power in a large-scale power plant, and small-scale devices were studied by Ref. [3], who studied a pilot scale 12 m high built in University of Zanjan, and by Ref. [4], who described a 2 m high device in Tehran. Among theoretical studies, analytical and numerical models were found in literature. The first theoretical model to predict the efficiency of a solar updraft tower is attributed to [5], who found a value of 1% for a height of 1000 m, and concluded that the device should be used for large scale power generation. Later, some analytical studies were developed to predict the performance of the device, validating the results by comparison with the Manzanares prototype [6]. evaluated the effects of the collector radius and chimney height on the power output [7]. estimated the power output and temperature configuration of the collector with and without a water storage system [8]. established a theoretical model for the diurnal behaviour of the incident solar radiation and the annual performance of a 100 MW solar chimney in Sinkiang, China [9]. evaluated the performance of solar chimney power plants in selected locations in Iran using a general and simplified mathematic model [10]. developed an analytical model to predict the exergetic losses and the exergetic efficiency of a solar chimney, based on experimental data from a small prototype built in Brazil [11]. developed a simple mathematical model for the performance of a solar chimney, as well as an economic analysis. The purpose was to investigate the feasibility of the technology under North Cyprus conditions, for the production of 30 MW. Numerical models were developed to predict the performance and main parameters of the airflow inside a solar

* Corresponding author.
E-mail addresses: cristiana@pucminas.br (C.B. Maia), agferreira@deii.cefetmg.br (A.G. Ferreira), cab35ezas@yahoo.com.br (L. Cabezas-Gómez), janainajocs@hotmail.com (J. de Oliveira Castro Silva), hanriot@pucminas.br (S. de Morais Hanriot).

http://dx.doi.org/10.1016/j.renene.2017.07.102
0960-1481/

updraft tower. The Manzanares project was used as a reference to validate the numerical results in Refs. [12–15]. Small scale devices were used as a reference in other works, such as [16–18]. Economic analyses were developed, as cited by Refs. [6, 19 and 20].

The original project was modified to incorporate innovative technologies. The solar updraft tower was used combined with geothermal sources ([19, 21 and 22]) and cooling towers to increase the thermal efficiency of a Rankine cycle ([23, 24]). The device was also used integrated with sea water desalination [25]. A novel solar updraft tower prototype was proposed by Ref. [26], consisting of a transpired solar collector, which uses metal in place of the traditional glazing covers. Ambient air enters through millions of perforations along the entire surface of the collector, not from the open perimeter.

Since the conversion efficiency of the solar energy into electric energy is very low, large structures are required to generate power at competitive prices [27]. Small devices can be used for other purposes, such as drying agricultural products [28] or natural ventilation [29]. Drying is the process of removing moisture from a product that is an essential process in the conservation of agricultural products and can be done in several ways. The use of solar radiation for drying is one of the oldest applications of solar energy [30]. Solar dryers used in agriculture for food and crop drying have proved to be very useful devices from the energy conservation point of view [31, 32]. present the state of various kinds of solar dryers widely used nowadays and the related technologies that can help improve existing solar dryers [28]. suggested the use of a small-scale solar updraft tower to dry agricultural products. The authors performed drying tests on coffee grains, bananas, and tomatoes and concluded that the device was technically viable. The drying of bananas, one of the major tropical fruits, is performed not only for preservation purposes, but also for modification in taste, flavour and texture to increase market value of the product [33]. In the literature, several works can be found on the drying of bananas, both experimental ([34–36]) and mathematical ([37, 38]).

According to [39], the use of energy as a parameter to identify and measure the benefits of energy systems can be misleading and confusing. Exergy analysis plays a vital rule in optimising drying conditions and improving the performance of drying systems [40]. Exergy can provide more useful and meaningful information, since it clearly identifies efficiency improvements and reductions in thermodynamic losses. Using exergy analysis, based on the first and second laws of thermodynamics, it is possible to infer the true potential of different kinds of energies [41, 42]. state that the performance of a drying system or drying process can be efficaciously tested and losses occurred in the components of energy systems can be separately evaluated through exergy analysis method. Most of the recent works developed on dryers make use of energy and exergy analysis ([43–47]). Also, the exergy analysis can be used to reduce the environmental impact of drying systems [48]. It has been shown [49] that an increase in exergy efficiency decreases the environmental impact and increases sustainability and vice versa.

According to [50], about 40 worth-noting experimental studies regarding solar updraft towers were developed, most related to small-scale devices. Although large structures are required to ensure high efficiencies, the studies were conducted to evaluate the solar updraft for power generation. This paper deals with the use of the airflow generated to dry agricultural products, which justifies the small dimensions of the device. An analysis of the thermodynamic behaviour of a solar updraft tower without load was performed by Ref. [10]. The authors presented an energetic and exergetic analysis of the airflow and concluded that the exergetic efficiency was very low, because the airflow generated was not used to drive a wind turbine or to dry agricultural products. In this paper, an energetic and exergetic analysis of the drying of bananas inside the same prototype solar updraft tower, located in Brazil, is presented. The use of the solar updraft tower to dry agricultural products is an innovative idea, as well as the exergetic analysis of the airflow inside the device.

2. Experimental methodology

An energetic and exergetic analysis of the airflow during the drying of bananas inside a solar updraft tower was performed. Environmental conditions and airflow parameters were monitored during four days of tests, in Brazil's spring. The bananas' drying was performed inside an experimental set-up constructed at the Federal University of Minas Gerais, Belo Horizonte, Brazil. The city has great solar energy potential due to its location (20°S latitude), with a yearly average daily total radiation of 16 MJ/m^2.day [51]. The experimental set-up of the solar updraft tower studied is shown schematically in Fig. 1, and there is a photograph of it in Fig. 2.

The total solar radiation incident on the solar updraft tower was measured using an Eppley Black and White Pyranometer Model 8–48. The temperatures were measured using K-type thermocouples, with the sensors positioned to measure ambient, ground, and outlet temperatures. Relative humidities (ambient and at the outlet) were measured using capacitive psychrometers, and the velocity in the tower outlet was measured using a Homis propeller anemometer. Measure points are illustrated in Fig. 3. After installing the sensors, the system was left to operate under normal weather conditions, and all measurements of the airflow were taken once every 10 min.

In order to predict errors and uncertainties, an uncertainty analysis was performed using the method described by Ref. [52]. The uncertainties of the sensors, based on the measured data, are presented in Table 1 with a confidence interval of 95%.

Drying tests of whole bananas inside the solar updraft tower were performed. Before beginning the drying tests, the products received a pretreatment and were divided into three samples. The first sample was used to assess the initial moisture content, the second was submitted to natural sun drying and the third sample was dried inside the device. The bananas were put to be dried on trays under the solar collector. The initial moisture content was 372% in a dry basis (d.b.) (corresponding to 79% in wet basis – w.b.). The time required for the bananas to achieve the final desired moisture content of 24% d.b. (corresponding to 20% in w.b.) was 139 h. Further details can be seen in Ref. [28].

3. Energy and exergy analyses

The science of thermodynamics is built primarily on the first and the second laws of thermodynamics. The first law deals with the quantity of energy and asserts that energy cannot be created or destroyed. The second law deals with the quality of energy and is concerned with the degradation of energy during a process, entropy generation, and the lost opportunities to do work [53]. The general energy and exergy analysis, developed according to the literature models ([54], [55], [10]), are given below.

3.1. Energy analysis

The mass and energy balances for any control volume at steady state can be expressed as follows:

$$\dot{m}_{ai} = \dot{m}_{ao} \tag{1}$$

where $\dot{m}_{ai}$ and $\dot{m}_{ao}$ represent the inlet and outlet mass flow rates, respectively.

The mass conservation for the moisture can be rewritten in

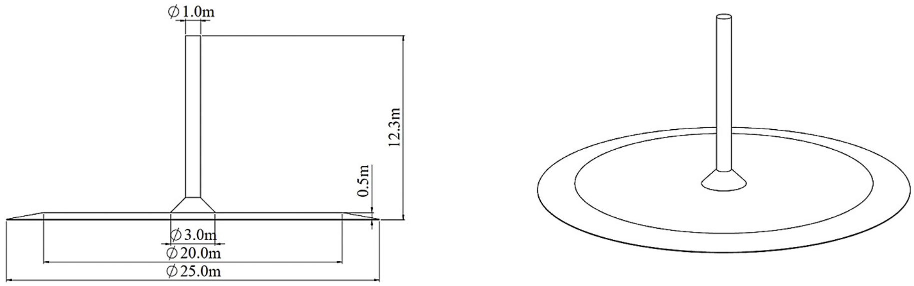

Fig. 1. Schematic of the prototype.

Fig. 2. Photograph of the prototype solar updraft tower.

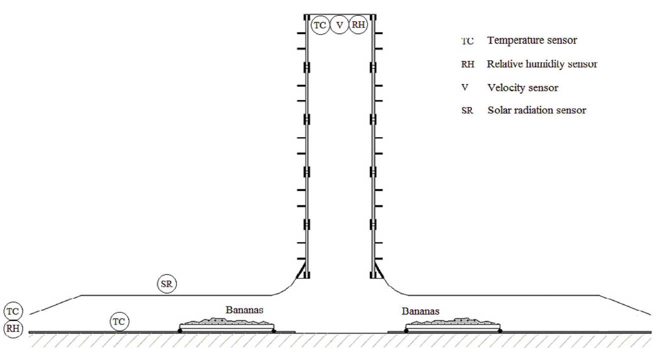

Fig. 3. Measure points.

Table 1
Uncertainty values associated with the measured values.

	Global uncertainty
Solar radiation	5%
Temperature	1.1 °C
Relative humidity	6%
Velocity	6%

terms of the mass flow of the moisture from the ground, $\dot{m}_{mp}$, and the inflow and outflow specific humidities, ω_{ai} and ω_{ao}, respectively, as:

$$\dot{m}_{ai}\omega_{ai} + \dot{m}_{mp} = \dot{m}_{ao}\omega_{ao} \tag{2}$$

The net heat rate, $\dot{Q}$, can be determined through a general energy balance.

$$\dot{Q} = \dot{m}_{ao}\left(h_{ao} + \frac{V_{ao}^2}{2}\right) - \dot{m}_{ai}\left(h_{ai} + \frac{V_{ai}^2}{2}\right) \tag{3}$$

The energy utilization rate is neglected, since there is no turbine in the system. V_{ai} and V_{ao} represent the air velocity in the inlet and outlet of the system, respectively. The specific enthalpies of the air in the inlet and outlet, h_{ai} and h_{ao}, were determined using the functions available in the EES (Engineering Equation Solver) software.

The thermal efficiency for the solar collector can be determined by Ref. [36].

$$\eta = \frac{\dot{m}_a c_p (T_{ao} - T_{ai})}{A_c I} \tag{4}$$

$\dot{m}_a$ is the mass flow rate of the dried air, T_{ai} and T_{ao} are the air temperatures in the inlet and outlet, respectively. C_p is the specific heat of the air, A_c is the collector area and I is the incident solar radiation.

3.2. Exergy analysis

The general exergy balance can be written as follows:

$$\sum \dot{E}x_{in} - \sum \dot{E}x_{out} = \sum \dot{E}x_{lost} \tag{5}$$

In equation (5), $\dot{E}x_{in}$, $\dot{E}x_{out}$, and $\dot{E}x_{lost}$ represent the exergy inflow, outflow, and loss, respectively. This equation can be also expressed as:

$$\dot{E}x_{heat} - \dot{E}x_{work} + \dot{E}x_{mass,in} - \dot{E}x_{mass,out} = \dot{E}x_{lost} \tag{6}$$

With the exergy flow rate due to the heat transfer given by:

$$\dot{E}x_{heat} = \left(1 - \frac{T_o}{T_k}\right)\dot{Q} \tag{7}$$

$\dot{Q}$ is the heat transfer rate through the boundary at temperature T_k at location k, and is the ground temperature. T_o represents the dead state temperature. For the system considered, the exergy rate due to work interactions $\dot{E}x_{work}$ can be neglected.

The exergy inflow $\dot{E}x_{mass,in}$ is only due to the airflow entering the system, and the exergy outflow $\dot{E}x_{mass,out}$ is due to the airflow leaving the system and the water removed, $\dot{E}x_w$.

$$\dot{E}x_{mass,in} = \dot{m}_{ai}\Psi_{ai} \tag{8}$$

$$\dot{E}x_{mass,out} = \dot{m}_{ao}\Psi_{ao} + \dot{E}x_w \tag{9}$$

where:

$$\dot{E}x_w = \dot{m}_{mp}\Psi_{wo} \tag{10}$$

Therefore, the exergy outflow is:

$$\dot{E}x_{mass,out} = \dot{m}_{ao}\Psi_{ao} + \dot{m}_{mp}\Psi_{wo} \tag{11}$$

The inlet and outlet specific flow exergies are calculated according to [56]:

$$\begin{aligned}\Psi_{ai} = {} & (C_{p,ai} + \omega_{ai}C_{p,v})\, T_o\left(\frac{T_{ai}}{T_o} - 1 - \ln\frac{T_{ai}}{T_o}\right) \\ & + (1 + 1.6078\omega_{ai})R_a T_o \ln\frac{P_{ai}}{P_o} \\ & + R_a T_o\left[(1 + 1.6078\omega_{ai})\ln\left(\frac{1 + 1.6078\omega_o}{1 + 1.6078\omega_{ai}}\right)\right. \\ & \left. + 1.6078\omega_{ai}\ln\left(\frac{\omega_{ai}}{\omega_o}\right)\right]\end{aligned} \tag{12}$$

$$\begin{aligned}\Psi_{ao} = {} & (C_{p,ao} + \omega_{ao}C_{p,v})\, T_o\left(\frac{T_{ao}}{T_o} - 1 - \ln\frac{T_{ao}}{T_o}\right) \\ & + (1 + 1.6078\omega_{ao})R_a T_o \ln\frac{P_{ao}}{P_o} \\ & + R_a T_o\left[(1 + 1.6078\omega_{ao})\ln\left(\frac{1 + 1.6078\omega_o}{1 + 1.6078\omega_{ao}}\right)\right. \\ & \left. + 1.6078\omega_{ao}\ln\left(\frac{\omega_{ao}}{\omega_o}\right)\right]\end{aligned} \tag{13}$$

where R_a is the ideal air constant, P_o is the dead state pressure, P_{ai} and P_{ao} are the air pressure in the inlet and outlet, respectively, and T_{ai} and T_{ao} are the air temperatures in the inlet and outlet, respectively. $C_{p,v}$ is the specific heat of the water vapour, and ω_o is the specific humidity of the flow in dead state.

The outlet specific flow exergy of the water, considered as an incompressible substance, assuming the air and water leave the system at the same temperature, T_{ao}, is given by:

$$\Psi_{wo} = C\left(T_{ao} - T_o - T_o\ln\frac{T_{ao}}{T_o}\right) \tag{14}$$

In the previous equation, C is the specific heat of water.

Therefore, exergy loss is given by:

$$\dot{E}x_{lost} = \left(1 - \frac{T_o}{T_k}\right)\dot{Q} + \dot{m}_{ai}\Psi_{ai} - \dot{m}_{ao}\Psi_{ao} - \dot{m}_{mp}\Psi_{wo} \tag{15}$$

The exergy efficiency ε is defined as the ratio of total exergy output to total exergy input:

$$\varepsilon = \frac{\dot{E}x_{out}}{\dot{E}x_{in}} = 1 - \frac{\dot{E}x_{lost}}{\dot{E}x_{in}} \tag{16}$$

Exergy is always evaluated with respect to a reference environment, the dead state. When a system is in thermodynamic equilibrium with the environment, the state of the system is called the dead state due to the fact that the exergy is zero. According to [54], dead state is an arbitrary reference state. When the dead state conditions are variable, the reference state may be defined as constant or variable. The analysis performed using the time-varying environmental temperature as the dead state temperature provides more realistic exergy analysis results than using a constant value [57].

4. Results and discussion

Fig. 4 presents the experimentally measured solar radiation incident on the device (total and diffuse components). For comparison, the extraterrestrial radiation calculated for each day is shown. It can be seen that the total and diffuse components of the solar radiation presented significantly lower values than the extraterrestrial radiation on the first and second days. Fig. 5 presents a comparison between data experimentally obtained in this work and experimental values from the literature [59] for the city of Belo Horizonte, Brazil, and it can be seen that both data sets have similar values. Sinda (Integrated Environmental Data) is a system of the Brazilian government that provides historical environmental data for several cities.

The air enters the system at ambient temperature. The inlet and airflow temperatures are directly related to the incident total solar radiation on the device, as can be seen in Figs. 4 and 6. On the first and second days, lower temperatures were recorded, since the solar radiation was lower. As expected, higher temperatures were found during the middle of the day, when the solar radiation is highest. Also, the ground surface temperature is higher than the outlet temperature, which is higher than inlet temperature.

When products are placed to be dried inside the solar updraft tower, it is important to monitor the relative humidity, since the amount of water removed from the products is affected by the ambient relative humidity: the lower the relative humidity, the higher the amount of water removed. Fig. 7 presents the ambient relative humidity for the drying tests, as well as ambient temperature. As expected, it can be seen that they behaved inversely; when the ambient temperature increased, relative humidity decreased. Furthermore, it can be seen that the solar radiation plays an important role on the behaviour of the relative humidity. Higher solar radiation levels result in lower relative humidity.

When drying processes are being studied, evaluating the behaviour of absolute humidity is important. Fig. 8 presents the absolute humidity at the inlet and outlet of the solar updraft tower. It can be seen that the outlet humidity is always higher than the inlet humidity, which indicates the device was able to remove water from the products. Fig. 8 also shows the difference between outlet and inlet humidities, which indicates the efficiency of the tower. By comparing Figs. 6 and 8, it can be seen water removal is higher when the airflow temperature is higher.

The airflow is generated by buoyancy forces caused by temperature gradients. Therefore, higher velocities and mass flow rates are obtained when higher solar radiation is available. Fig. 9 presents the mass flow rate inside the solar updraft tower. It can be seen that

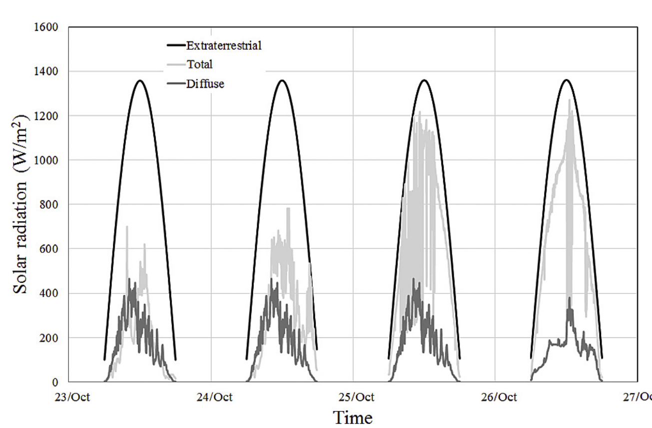

Fig. 4. Extraterrestrial radiation and incident solar radiation on the device.

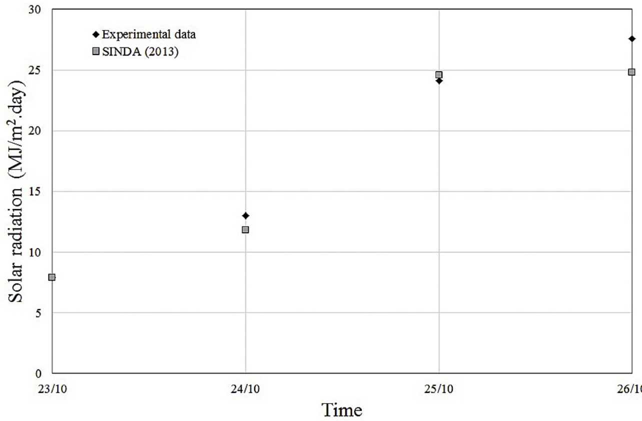

Fig. 5. Comparison between experimental data and literature data.

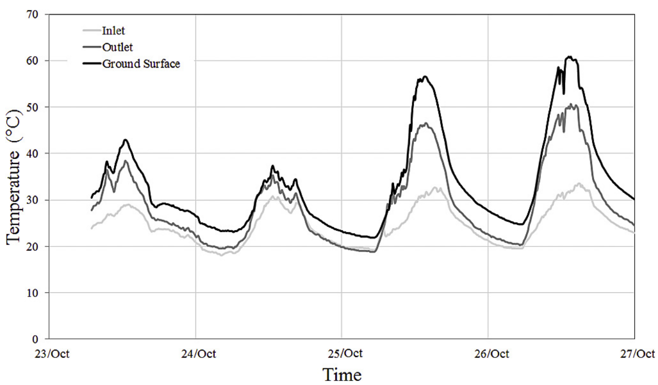

Fig. 6. Inlet, outlet, and ground surface temperatures.

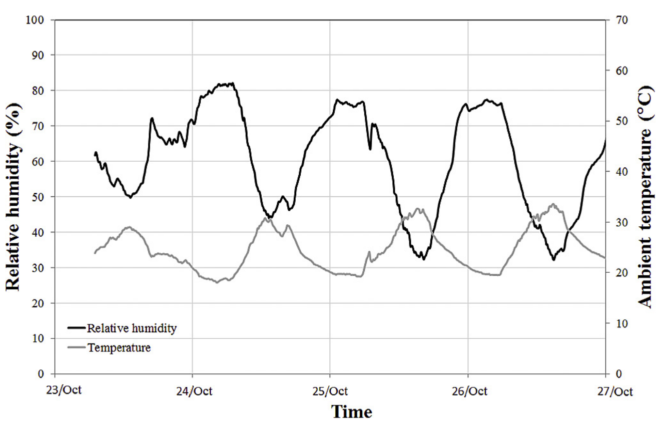

Fig. 7. Ambient temperature and relative humidity.

the higher values are found for the third and fourth days, when solar radiation and temperatures are higher. Moreover, it is worth noting that the solar updraft tower is able to generate a hot airflow even at night, when there is no incidence of solar radiation incident. When the temperature of the airflow is higher than the temperature of the deeper layers of the ground, the heat is transferred to the ground, and stored. At night, when the temperature of the airflow is lower, the heat is transferred in the opposite way [27]. Therefore, the airflow temperature is higher than ambient temperature (Fig. 6) and there is an uninterrupted functioning of the device.

Based on experimental data, it was possible to determine the

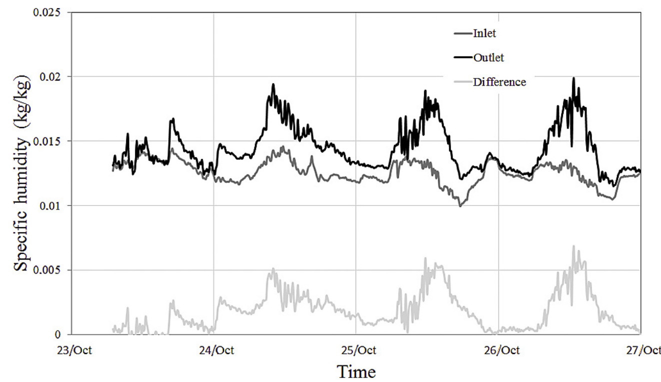

Fig. 8. Inlet and outlet specific humidity.

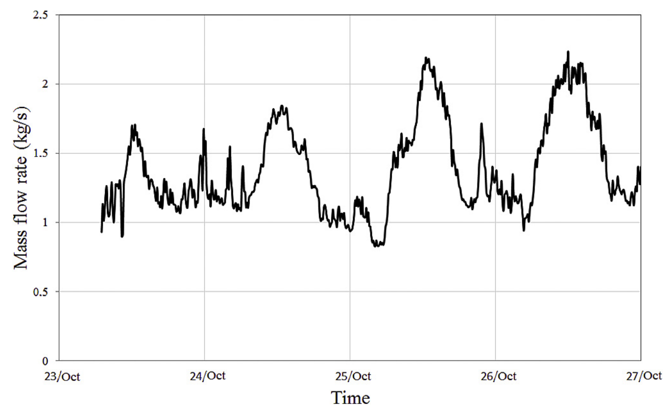

Fig. 9. Mass flow rate of the airflow in the chimney.

total heat absorbed by the airflow (Eq. (3)), which is presented in Fig. 10. This heat followed the same general behaviour as the other parameters, higher when there is a higher incidence of solar radiation.

Bananas were put inside the solar updraft tower to be dried. The bananas required approximately 139 h to reduce the initial moisture content from 372% to 24% (dry basis). During the drying period, the daily ambient air temperature and relative humidity averages were (24.5 ± 1.1)°C and (61 ± 4)%, respectively, and the average solar radiation was (459 ± 23) W/m^2 at a mass flow rate of (1.4 ± 0.1) kg/s, as shown in Figs. 4, 6 and 7. A plot showing the drying of the bananas is shown in Fig. 11 along with one for natural

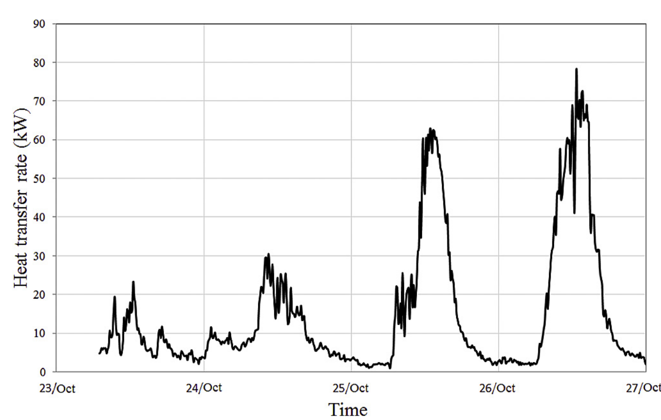

Fig. 10. Heat transfer rate absorbed by the airflow.

sun drying. It is observed that the products exposed directly to the sun required 178 h to achieve the same final moisture content of 24% (d.b.).

The collector efficiency was about 12%, for an average solar radiation of (459 ± 23) W/m^2, and average inlet and outlet temperatures of (24.5 ± 1.1)°C and (29.1 ± 1.1)°C, respectively [36]. used an indirect type solar dryer for banana drying, and reported a collector efficiency of 31.50%, for an average solar radiation of 724 W/m^2, and average inlet and outlet temperatures of 42 °C and 62 °C, respectively. The smaller value obtained in the solar updraft tower can be attributed to the larger collector area used in the efficiency equation and to the lower values obtained for incident solar radiation and, therefore, airflow temperature [33]. used a PV-ventilated solar greenhouse dryer to dry bananas. The bananas took 4 days to reduce the relative humidity (wet basis) from 70% to 24%, with solar radiation levels varying from 198 W/m^2 to 1080 W/m^2. Considering that this dryer used three DC fans operated by a 50 W PV module, and the airflow in the solar updraft tower was generated only by natural convection, the solar updraft tower presented good results. In this device, the bananas required 139 h to reduce the relative humidity (wet basis) from 79% to 20%.

The exergy rates over the time can be seen in Fig. 12. The behaviour of the exergy rates was a consequence of the changes in the incident solar radiation and the resulting heat transfer rates. For the first and second days, the incident solar radiation was very low, resulting in lower exergy rates. It can be also noticed that the most significant term is the exergy rate due to the heat transfer. The water removed from the bananas was small, resulting in low values for the exergy rate due to the water removed, not representative when compared to $\dot{E}x_{heat}$. and $\dot{E}x_{out}$. Since the dead state temperature is the inlet (ambient) temperature, the exergy inflow is always null.

The lost exergy is the difference between inlet and outlet exergy flows. As can be seen in Fig. 13, the general behaviour is similar to that of the exergy rates, with lower values for the first and second days.

According to [30], during the drying of any product, the drying rate usually has three different phases: an initial constant-rate period, a falling rate period, and the second part of falling rate period. In the second and third parts, the drying rate decreases and a lower amount of energy is used to dry the products. In the third and fourth days, most of the water had already been removed, and the drying rate was decreasing. Since less energy was used, the exergy lost increased.

Exergy efficiency is an indicator of the quality level of the converted energy. According to [58], this parameter for solar systems is

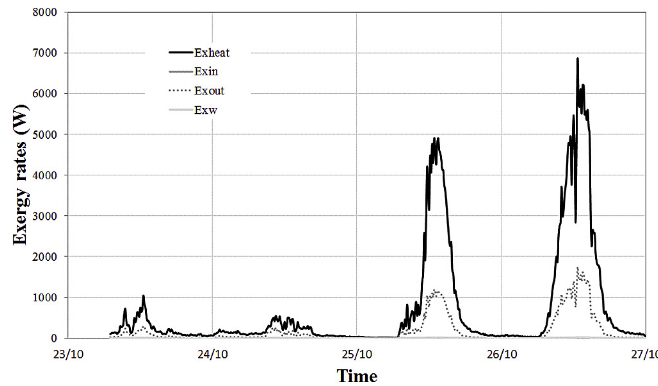

Fig. 12. Exergy rates as a function of drying time.

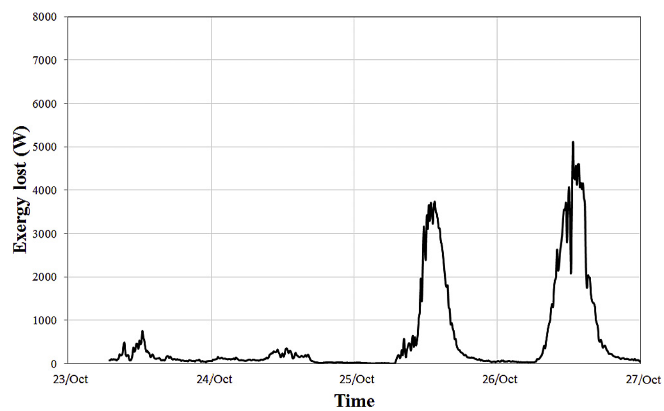

Fig. 13. Exergy losses by the airflow as a function of drying time.

highly dependent on the daily solar radiation and the radiation intensity. Fig. 14 presents the exergy efficiency of the drying process. It can be seen that the efficiency is higher for the first and second days, when the solar radiation was lower. It should be noted that this happened even when the solar radiation was higher on the last two days.

The efficiencies obtained for the drying of bananas inside the solar updraft tower can be compared to the efficiencies obtained without any load inside the device, presented in Ref. [10]. In the first work, an average efficiency value of 20% was found for an average total solar radiation value of (17.5 ± 0.9) MJ/m^2.day. In the present work, an average value of 27.3% was found for an average

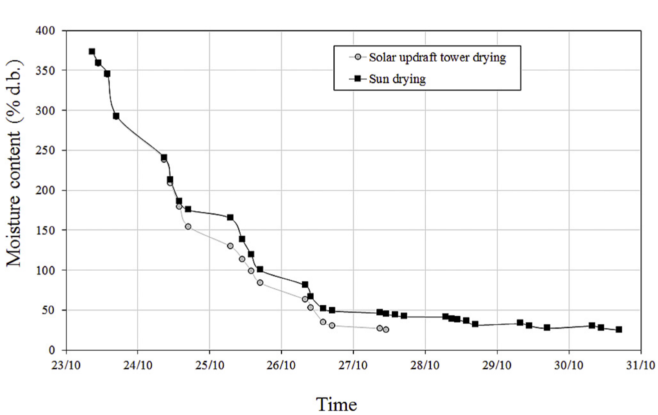

Fig. 11. Comparison of drying curves of bananas dried inside the solar updraft tower and natural sun drying.

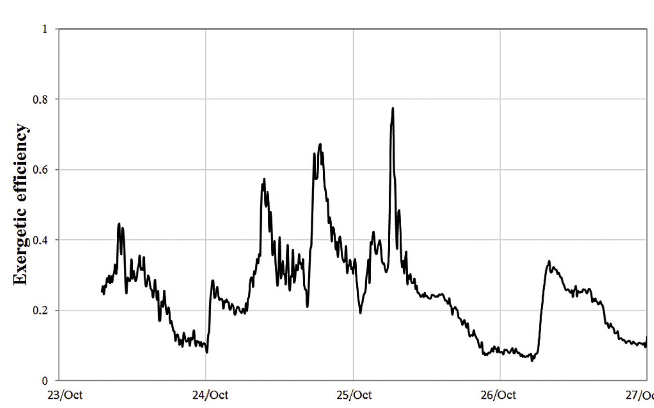

Fig. 14. Exergy efficiency of the drying process as a function of drying time.

total solar radiation value of (20.1 ± 1.0) MJ/m^2.day. When the solar updraft tower is operating with no load, the hot airflow generated was not used to dry any products or to drive a turbine, thus it was lost, reducing the exergy efficiency. When the bananas were put inside the device, part of the energy was used to dry the products, reducing the exergy losses and increasing the exergy efficiency.

5. Conclusions

An energetic and exergetic evaluation of the drying of bananas inside a solar updraft tower was performed. Ambient parameters were evaluated in order to determine their influence on the exergy rates, exergetic efficiency and on the drying and the heat transferred to the airflow. The incident solar radiation plays an important role in the process, since it is the driving force in generating the hot airflow. The higher the solar radiation, the higher the airflow temperatures and mass flow rates, and the higher the heat transfer rates and the water removed by the solar updraft tower.

The performance of the solar updraft tower as a dryer was compared to other dryers. It was found that the collector efficiency presented lower values, attributed to the lower levels of solar radiation incident during the tests and to the larger collector area, when compared to usual dryers. Furthermore, the drying time was compatible to dryers assisted by PV modules.

The average exergetic efficiency was 27% at an average solar radiation level of about 450 W/m^2 and an ambient temperature of 24.5 °C. The average airflow temperature and mass flow rate were 29 °C and 1.4 kg/s, respectively. The airflow temperature reached a maximum of 51 °C. It was compared the exergetic efficiency of the drying process with the exergetic efficiency of the solar updraft tower operating without load, and it was observed a significant increase in the exergetic efficiency, from 20% to 27%.

Acknowledgements

The authors are thankful to UFMG, PUC Minas, FAPEMIG, CAPES and CNPq.

References

[1] W. Haaf, {SOLAR} {CHIMNEYS} - {PART} {II:} {PRELIMINARY} {TEST} {RESULTS} {FROM} {THE} {MANZANARES} {PILOT} {PLANT.}, Int. J. Sol. Energy 2 (1984) 141–161, http://dx.doi.org/10.1080/01425918408909921.
[2] M. Najmi, A. Nazari, H. Mansouri, G. Zahedi, Feasibility study on optimization of a typical solar chimney power plant, Heat Mass Transf. 48 (2012) 475–485, http://dx.doi.org/10.1007/s00231-011-0894-5.
[3] A.B. Kasaeian, E. Heidari, S.N. Vatan, Experimental investigation of climatic effects on the efficiency of a solar chimney pilot power plant, Renew. Sustain. Energy Rev. 15 (2011) 5202–5206, http://dx.doi.org/10.1016/j.rser.2011.04.019.
[4] M. Ghalamchi, A. Kasaeian, M. Ghalamchi, Experimental study of geometrical and climate effects on the performance of a small solar chimney, Renew. Sustain. Energy Rev. 43 (2015) 425–431, http://dx.doi.org/10.1016/j.rser.2014.11.068.
[5] L.B. Mullett, {SOLAR} {CHIMNEY} - {OVERALL} {EFFICIENCY}, {DESIGN} {AND} {PERFORMANCE.}, Int. J. Ambient. Energy 8 (1987) 35–40, http://dx.doi.org/10.1080/01430750.1987.9675512.
[6] J.yin Li, P. hua Guo, Y. Wang, Effects of collector radius and chimney height on power output of a solar chimney power plant with turbines, Renew. Energy 47 (2012) 21–28, http://dx.doi.org/10.1016/j.renene.2012.03.018.
[7] Y.J. Choi, D.H. Kam, Y.W. Park, Y.H. Jeong, Development of analytical model for solar chimney power plant with and without water storage system, Energy 112 (2016) 200–207, http://dx.doi.org/10.1016/j.energy.2016.06.023.
[8] P. Guo, J. Li, Y. Wang, Numerical simulations of solar chimney power plant with radiation model, Renew. Energy 62 (2014) 24–30, http://dx.doi.org/10.1016/j.renene.2013.06.039.
[9] R. Sangi, Performance evaluation of solar chimney power plants in Iran, Renew. Sustain. Energy Rev. 16 (2012) 704–710, http://dx.doi.org/10.1016/j.rser.2011.08.035.
[10] C.B. Maia, J.O. Castro Silva, L. Cabezas-Gómez, S.M. Hanriot, A.G. Ferreira, Energy and exergy analysis of the airflow inside a solar chimney, Renew. Sustain. Energy Rev. 27 (2013) 350–361, http://dx.doi.org/10.1016/j.rser.2013.06.020.
[11] C.O. Okoye, U. Atikol, A parametric study on the feasibility of solar chimney power plants in North Cyprus conditions, Energy Convers. Manag. 80 (2014) 178–187, http://dx.doi.org/10.1016/j.enconman.2014.01.009.
[12] G. Xu, T. Ming, Y. Pan, F. Meng, C. Zhou, Numerical analysis on the performance of solar chimney power plant system, Energy Convers. Manag. 52 (2011) 876–883, http://dx.doi.org/10.1016/j.enconman.2010.08.014.
[13] R. Sangi, M. Amidpour, B. Hosseinizadeh, Modeling and numerical simulation of solar chimney power plants, Sol. Energy 85 (2011) 829–838, http://dx.doi.org/10.1016/j.solener.2011.01.011.
[14] P. Guo, J. Li, Y. Wang, Y. Wang, Numerical study on the performance of a solar chimney power plant, Energy Convers. Manag. 105 (2015) 197–205, http://dx.doi.org/10.1016/j.enconman.2015.07.072.
[15] N. Fathi, S.S. Aleyasin, P. Vorobieff, Numerical-analytical assessment on Manzanares prototype, Appl. Therm. Eng. 102 (2016) 243–250, http://dx.doi.org/10.1016/j.applthermaleng.2016.03.133.
[16] M. Lebbi, T. Chergui, H. Boualit, I. Boutina, Influence of geometric parameters on the hydrodynamics control of solar chimney, Int. J. Hydrogen Energy 39 (2014) 15246–15255, http://dx.doi.org/10.1016/j.ijhydene.2014.04.215.
[17] A. Kasaeian, M. Ghalamchi, M. Ghalamchi, Simulation and optimization of geometric parameters of a solar chimney in Tehran, Energy Convers. Manag. 83 (2014) 28–34, http://dx.doi.org/10.1016/j.enconman.2014.03.042.
[18] K. Milani Shirvan, S. Mirzakhanlari, M. Mamourian, N. Abu-Hamdeh, Numerical investigation and sensitivity analysis of effective parameters to obtain potential maximum power output: a case study on Zanjan prototype solar chimney power plant, Energy Convers. Manag. 136 (2017) 350–360, http://dx.doi.org/10.1016/j.enconman.2016.12.081.
[19] F. Cao, H. Li, Q. Ma, L. Zhao, Design and simulation of a geothermal-solar combined chimney power plant, Energy Convers. Manag. 84 (2014) 186–195, http://dx.doi.org/10.1016/j.enconman.2014.04.015.
[20] E. Gholamalizadeh, M.-H. Kim, Thermo-economic triple-objective optimization of a solar chimney power plant using genetic algorithms, Energy 70 (2014) 204–211, http://dx.doi.org/10.1016/j.energy.2014.03.115.
[21] Z. Zou, Z. Guan, H. Gurgenci, Y. Lu, Solar enhanced natural draft dry cooling tower for geothermal power applications, Sol. Energy 86 (2012) 2686–2694, http://dx.doi.org/10.1016/j.solener.2012.06.003.
[22] Z. Zou, S. He, Modeling and characteristics analysis of hybrid cooling-tower-solar-chimney system, Energy Convers. Manag. 95 (2015) 59–68, http://dx.doi.org/10.1016/j.enconman.2015.01.085.
[23] A. Zandian, M. Ashjaee, The thermal efficiency improvement of a steam Rankine cycle by innovative design of a hybrid cooling tower and a solar chimney concept, Renew. Energy 51 (2013) 465–473, http://dx.doi.org/10.1016/j.renene.2012.09.051.
[24] B. Ghorbani, M. Ghashami, M. Ashjaee, H. Hosseinzadegan, Electricity production with low grade heat in thermal power plants by design improvement of a hybrid dry cooling tower and a solar chimney concept, Energy Convers. Manag. 94 (2015) 1–11, http://dx.doi.org/10.1016/j.enconman.2015.01.044.
[25] L. Zuo, Y. Yuan, Z. Li, Y. Zheng, Experimental research on solar chimneys integrated with seawater desalination under practical weather condition, Desalination 298 (2012) 22–33, http://dx.doi.org/10.1016/j.desal.2012.05.001.
[26] D. Eryener, J. Hollick, H. Kuscu, Thermal performance of a transpired solar collector updraft tower, Energy Convers. Manag. 142 (2017) 286–295, http://dx.doi.org/10.1016/j.enconman.2017.03.052.
[27] C.B. Maia, A.G. Ferreira, R.M. Valle, M.F.B. Cortez, Theoretical evaluation of the influence of geometric parameters and materials on the behavior of the airflow in a solar chimney, Comput. Fluids 38 (2009) 625–636, http://dx.doi.org/10.1016/j.compfluid.2008.06.005.
[28] A.G. Ferreira, C.B. Maia, M.F.B. Cortez, R.M. Valle, Technical feasibility assessment of a solar chimney for food drying, Sol. Energy 82 (2008) 198–205, http://dx.doi.org/10.1016/j.solener.2007.08.002.
[29] R. Khanal, C. Lei, An experimental investigation of an inclined passive wall solar chimney for natural ventilation, Sol. Energy 107 (2014) 461–474, http://dx.doi.org/10.1016/j.solener.2014.05.032.
[30] V. Belessiotis, E. Delyannis, Solar drying, Sol. Energy 85 (2011) 1665–1691, http://dx.doi.org/10.1016/j.solener.2009.10.001.
[31] S. Vijayavenkataraman, S. Iniyan, R. Goic, A review of solar drying technologies, Renew. Sustain. Energy Rev. 16 (2012) 2652–2670, http://dx.doi.org/10.1016/j.rser.2012.01.007.
[32] A.G.M.B. Mustayen, S. Mekhilef, R. Saidur, Performance study of different solar dryers: a review, Renew. Sustain. Energy Rev. 34 (2014) 463–470, http://dx.doi.org/10.1016/j.rser.2014.03.020.
[33] S. Janjai, N. Lamlert, P. Intawee, B. Mahayothee, B.K. Bala, M. Nagle, J. Müller, Experimental and simulated performance of a PV-ventilated solar greenhouse dryer for drying of peeled longan and banana, Sol. Energy 83 (2009) 1550–1565, http://dx.doi.org/10.1016/j.solener.2009.05.003.
[34] B.M.A. Amer, M.A. Hossain, K. Gottschalk, Design and performance evaluation of a new hybrid solar dryer for banana, Energy Convers. Manag. 51 (2010) 813–820, http://dx.doi.org/10.1016/j.enconman.2009.11.016.
[35] R.F. Zabalaga, C.I.A. La Fuente, C.C. Tadini, Experimental determination of thermophysical properties of unripe banana slices (Musa cavendishii) during convective drying, J. Food Eng. 187 (2016) 62–69, http://dx.doi.org/10.1016/j.jfoodeng.2016.04.020.
[36] A. Lingayat, V.P. Chandramohan, V.R.K. Raju, Design, development and performance of indirect type solar dryer for banana drying, Energy Procedia 109

(2017) 409–416, http://dx.doi.org/10.1016/j.egypro.2017.03.041.
[37] B. Hadrich, N. Kechaou, Mathematical modeling and simulation of shrunk cylindrical material's drying kinetics-Approximation and application to banana, Food Bioprod. Process 87 (2009) 96–101, http://dx.doi.org/10.1016/j.fbp.2008.06.003.
[38] W.P. Da Silva, A.F. Rodrigues, C.M.D.P.S. E Silva, D.S. De Castro, J.P. Gomes, Comparison between continuous and intermittent drying of whole bananas using empirical and diffusion models to describe the processes, J. Food Eng. 166 (2015) 230–236, http://dx.doi.org/10.1016/j.jfoodeng.2015.06.018.
[39] M.A. Rosen, I. Dincer, M. Kanoglu, Role of exergy in increasing efficiency and sustainability and reducing environmental impact, Energy Policy 36 (2008) 128–137, http://dx.doi.org/10.1016/j.enpol.2007.09.006.
[40] D.K. Rabha, P. Muthukumar, C. Somayaji, Energy and exergy analyses of the solar drying processes of ghost chilli pepper and ginger, Renew. Energy 105 (2017) 764–773, http://dx.doi.org/10.1016/j.renene.2017.01.007.
[41] N.L. Panwar, S.C. Kaushik, S. Kothari, A review on energy and exergy analysis of solar dying systems, Renew. Sustain. Energy Rev. 16 (2012) 2812–2819, http://dx.doi.org/10.1016/j.rser.2012.02.053.
[42] Z. Erbay, A. Hepbasli, Assessment of cost sources and improvement potentials of a ground-source heat pump food drying system through advanced exergoeconomic analysis method, Energy 127 (2017) 502–515, http://dx.doi.org/10.1016/j.energy.2017.03.148.
[43] N. Colak, A. Hepbasli, Performance analysis of drying of green olive in a tray dryer, J. Food Eng. 80 (2007) 1188–1193, http://dx.doi.org/10.1016/j.jfoodeng.2006.09.017.
[44] N.A. Aviara, L.N. Onuoha, O.E. Falola, J.C. Igbeka, Energy and exergy analyses of native cassava starch drying in a tray dryer, Energy 73 (2014) 809–817, http://dx.doi.org/10.1016/j.energy.2014.06.087.
[45] A. Fudholi, K. Sopian, M.H. Yazdi, M.H. Ruslan, M. Gabbasa, H.A. Kazem, Performance analysis of solar drying system for red chili, Sol. Energy 99 (2014) 47–54, http://dx.doi.org/10.1016/j.solener.2013.10.019.
[46] A.K. Sekone, Y.-Y. Hung, C.-T. Yeh, M.-T. Lee, Experimental study and analysis of porous thin plate drying in a convection dryer, Int. Commun. Heat. Mass Transf. 68 (2015) 200–207, http://dx.doi.org/10.1016/j.icheatmasstransfer.2015.08.019.
[47] W. Amjad, O. Hensel, A. Munir, A. Esper, B. Sturm, Thermodynamic analysis of drying process in a diagonal-batch dryer developed for batch uniformity using potato slices, J. Food Eng. 169 (2016) 238–249, http://dx.doi.org/10.1016/j.jfoodeng.2015.09.004.
[48] M. Aghbashlo, H. Mobli, S. Rafiee, A. Madadlou, A review on exergy analysis of drying processes and systems, Renew. Sustain, Energy Rev. 22 (2013) 1–22, http://dx.doi.org/10.1016/j.rser.2013.01.015.
[49] I. Dincer, Exergy as a potential tool for sustainable drying systems, Sustain. Cities Soc. 1 (2011) 91–96, http://dx.doi.org/10.1016/j.scs.2011.04.001.
[50] A.B. Kasaeian, S. Molana, K. Rahmani, D. Wen, A review on solar chimney systems, Renew. Sustain. Energy Rev. 67 (2017) 954–987, http://dx.doi.org/10.1016/j.rser.2016.09.081.
[51] C. Tiba, Atlas Solarimétrico do Brasil: Banco de Dados Terrestres, Atlas Solarimétrico Do Bras, vol. 1, 2000, p. 111. http://www.cresesb.cepel.br/publicacoes.
[52] R.J. Moffat, Describing the uncertainties in experimental results, Exp. Therm. Fluid Sci. 1 (1988) 3–17, http://dx.doi.org/10.1016/0894-1777(88)90043-X.
[53] Y.A. Cengel, M.A. Boles, Thermodynamics an Engineering Approach, 2013, http://dx.doi.org/10.1017/CBO9781107415324.004.
[54] A. Hepbasli, A key review on exergetic analysis and assessment of renewable energy resources for a sustainable future, Renew. Sustain. Energy Rev. 12 (2008) 593–661, http://dx.doi.org/10.1016/j.rser.2006.10.001.
[55] A.R. Celma, F. Cuadros, Energy and exergy analyses of OMW solar drying process, Renew. Energy 34 (2009) 660–666, http://dx.doi.org/10.1016/j.renene.2008.05.019.
[56] M.G. Alpuche, C. Heard, R. Best, J. Rojas, Exergy analysis of air cooling systems in buildings in hot humid climates, Appl. Therm. Eng. 25 (2005) 507–517, http://dx.doi.org/10.1016/j.applthermaleng.2004.07.006.
[57] C. Onan, D.B. Ozkan, S. Erdem, Exergy analysis of a solar assisted absorption cooling system on an hourly basis in villa applications, Energy 35 (2010) 5277–5285, http://dx.doi.org/10.1016/j.energy.2010.07.037.
[58] R. Saidur, G. Boroumandjazi, S. Mekhlif, M. Jameel, Exergy analysis of solar energy applications, Renew. Sustain. Energy Rev. 16 (2012) 350–356, http://dx.doi.org/10.1016/j.rser.2011.07.162 (Web references).
[59] Sinda, Sistema Integrado de Dados Ambientais, 2013. Available at: http://sinda.crn2.inpe.br. Accessed October 5 2016.